

X-ray emission from an X-pinch and its applications

R. LIU, X. ZOU, X. WANG, N. ZENG, AND L. HE

Department of Electrical Engineering, Tsinghua University, Beijing, China

(RECEIVED 20 April 2008; ACCEPTED 15 June 2008)

Abstract

The temporal and spatial X-ray emission from PPG-X, an X-pinch driven by pulsed power generator, was studied by using diamond photo-conducting detectors and pinhole cameras. It was found that the X-ray pulse usually consists of two sub-nanosecond peaks with a time interval of about 0.5 ns, these two X-ray peaks are consistent with two point sources of X-ray recorded with pinhole camera. The total X-ray energy changes from shot to shot and is averaged to be 0.35 J for $h\nu > 1.5$ keV. The size of the X-ray point source is in the range from 100 μm to 5 μm , decreasing rapidly with the increase of the photon energy. The X-pinch was used as X-ray source for backlighting the electrical explosion of single wire and for phase-contrast imaging of a mosquito.

Keywords: X-pinch; X-ray radiography; X-ray source

1. INTRODUCTION

Pulsed power generators, Z-pinch and X-pinch are very effective tools to generate large amounts of X-rays for various applications (Liu *et al.*, 2006; Liu *et al.*, 2007a; Liu *et al.*, 2007b; Orlov *et al.*, 2007; Spielman & De Groot, 2001; Winterberg, 2006). An X-pinch is produced with a high and pulse current flowing through two or more fine wires that cross and touch at a single point, forming an “X” shape. Due to the action of the magnetic field produced by the current, the plasma is imploded and one or more bright spots that emit intense X-ray bursts are formed at the position very near the crossing point of the wires. X-pinch plasma could be used as an intensive and sub-nanoseconds X-ray point source and may find many potential applications in biology, clinical science, high-energy density physics, and sub-micron lithography (Cosslett *et al.*, 1960; Kantsyrev *et al.*, 2004; Plidden *et al.*, 1994). In this article, we present the results of temporal and spatial measurements of X-ray emission from PPG-X (Liu *et al.*, 2008), an X-pinch driven by a pulsed power generator PPG-1 (Zou *et al.*, 2006), and we show that PPG-X is a good X-ray source for backlighting the electrical explosion of single wire, and for phase-contrast imaging of weakly X-ray absorbing objects such as a mosquito.

2. EXPERIMENTAL SETUP

The X-pinch we used was powered by PPG-1, a pulsed power generator that consists of a 1.2 MV Marx generator, a 1.25 Ω pulse forming line, a pressurized SF₆/N switch, a 1.25 Ω pulse transmission line. PPG-1 was designed to be capable of delivering to a matched load a pulse current of 400 kA in amplitude and 100 ns in pulse width (FWHM). For driving a two-wire X-pinch load, PPG-1 was usually operated with an output current of 200 kA. In our experiment, two 25- μm or 50- μm Mo wires were used as X-pinch load that connects with the anode and the cathode. The distance between the anode and the cathode is 16 mm.

The time-resolved X-ray emission was measured with three X-ray photo-conducting detectors (PCDs) each using a diamond (3 mm \times 1 mm \times 1 mm) as an X-ray sensor. The PCDs from Alameda Applied Science Corporation (AASC) were calibrated to have a sensitivity of 5×10^4 A/W at a biasing voltage of 100 V. Different filters were used for different PCDs and thus the X-rays with different minimum photon energies were measured. PCD1 was covered by a 50- μm thick Be filter for measuring X-rays with $h\nu > 1.5$ keV, PCD2 by a 12.5- μm thick Ti filter for X-rays with $h\nu > 2.5$ keV, and PCD3 by a 20- μm Al filter for X-rays with $h\nu > 4$ keV. Being housed in vacuum tubes, all PCDs were installed at a distance of 820 mm from the X-ray source, the crossing point of the wires. The positions of all PCDs are at a plane perpendicular to the axis of X-pinch electrodes and passes through the crossing point of the wires. If we define a cylinder coordinate

Address correspondence and reprint request to: Xinxin Wang, Department of Electrical Engineering, Tsinghua University, Beijing 100084, China.
E-mail: wangxx@mail.tsinghua.edu.cn

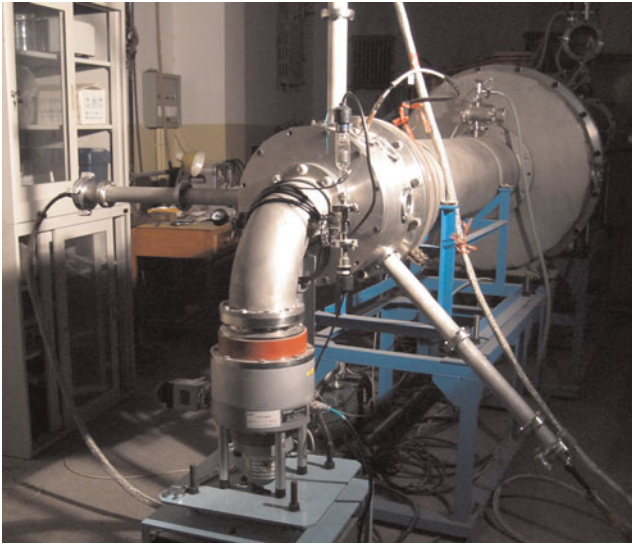


Fig. 1. (Color online) Three PCDs are housed in three long vacuum tubes.

system (Z, r, φ) , whose origin is the crossing point of the wires and whose Z axis is the axis of the electrodes, the coordinates for PCDs are PCD1 ($Z = 0, r = 820 \text{ mm}, \varphi = 0^\circ$), PCD2 ($Z = 0, r = 820 \text{ mm}, \varphi = 90^\circ$) and PCD3 ($Z = 0, r = 820 \text{ mm}, \varphi = 225^\circ$), as shown in Figure 1. The pattern of the X-ray source was recorded on X-ray sensitive film (KODAK: BioMax-MS) by using an $8\text{-}\mu\text{m}$ aperture pinhole camera. The distances from the source to the pinhole and from the pinhole to the film are 80 mm and 440 mm, respectively, which correspond to a geometric magnification of 5.5.

3. RESULTS AND DISCUSSIONS

3.1. Temporal Behavior of the X-ray Emission

Figure 2 is the typical signal of X-ray from an X-pinch using two $25\text{-}\mu\text{m}$ Mo wires as the load. As a time reference, the waveform of the load current is also recorded. From Figure 2a, we could see that the narrow X-ray pulse appears far ahead of the load current maximum that is about 200 kA, indicating that the load mass of two $25\text{-}\mu\text{m}$ Mo wires is too small for a 200 kA current. If the waveform of the narrow X-ray pulse is expanded with time, as shown in Figure 2b, we see a single pulse with a pulse width of 1.2 ns (FWHM) that is much larger than what we expected. The reason for this larger pulse width of X-ray lies in the digital oscilloscope, Tektronix TDS5034B, with which the waveforms in Figure 2 were recorded. The bandwidth and the sampling rate for TDS5034B are 350 MHz and 2.5 GS/s, respectively, which mean 1 ns has only 2.5 sampling points. Obviously, TDS5034B is not fast enough to record a sub-nanosecond pulse.

When TDS5034B is replaced by a much faster oscilloscope, Lecroy SDA6020, with a bandwidth of 6 GHz, and a sampling rate of 20 GS/s, the recorded X-ray pulses are totally different,

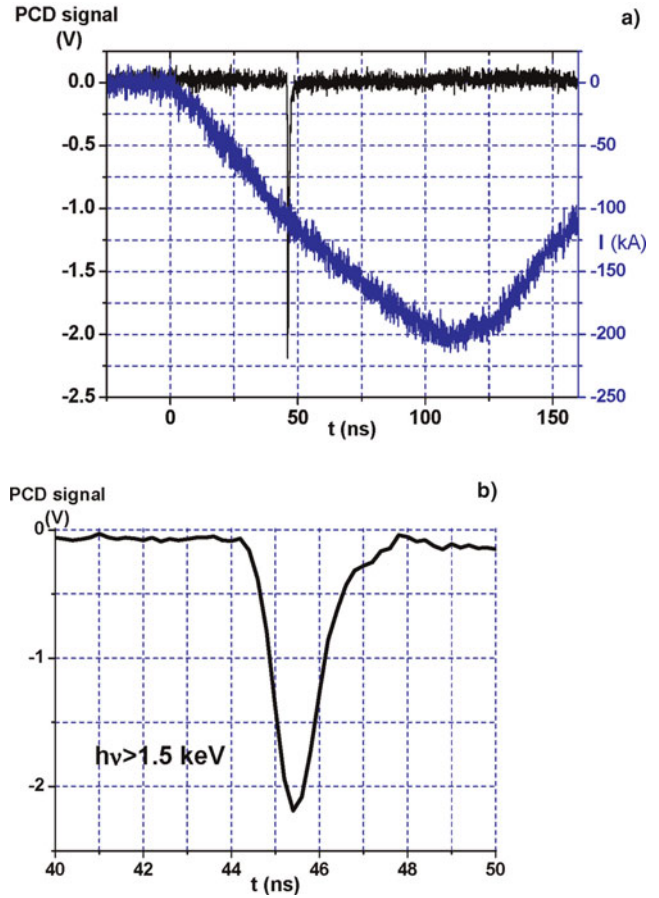


Fig. 2. (Color online) The typical result obtained from the experiments using two $25\text{-}\mu\text{m}$ Mo wires as X-pinch load: (a) The waveforms of the X-ray pulse and the load current, (b) the time expansion of the X-ray pulse.

as shown in Figure 3. The X-ray pulse usually consists of two sub-nanosecond peaks, so close to each other in time that they could only be separated by a very fast oscilloscope such as SDA6020. It was found that the amplitude of the X-ray signal decreases rapidly as the photon energy of the measured X-rays increases, i.e., 8 V for $h\nu > 1.5 \text{ keV}$, 1.2 V for $h\nu > 2.5 \text{ keV}$, and 0.7 V for $h\nu > 4 \text{ keV}$.

In order to study whether the X-ray emission from the X-pinch is isotropic, we used the same filter, $50\text{-}\mu\text{m}$ thick Be, in front of 3 PCDs. From Figure 4 we could see that the X-ray pulses recorded by these 3 PCDs are more or less the same for a same shot of X-pinch discharge. We concluded that the X-ray emission is isotropic in the plane in which PCDs are installed.

The X-ray energy deposited on one PCD could be calculated using the following equation:

$$W_{PCD} = \frac{1}{R \cdot S} \int_0^\infty V_{PCD}(t) \cdot dt, \quad (1)$$

where S is the sensitivity of the PCD; $V_{PCD}(t)$ is the output voltage of PCD; R is the PCD voltage sampling resistor through which the PCD current flows.

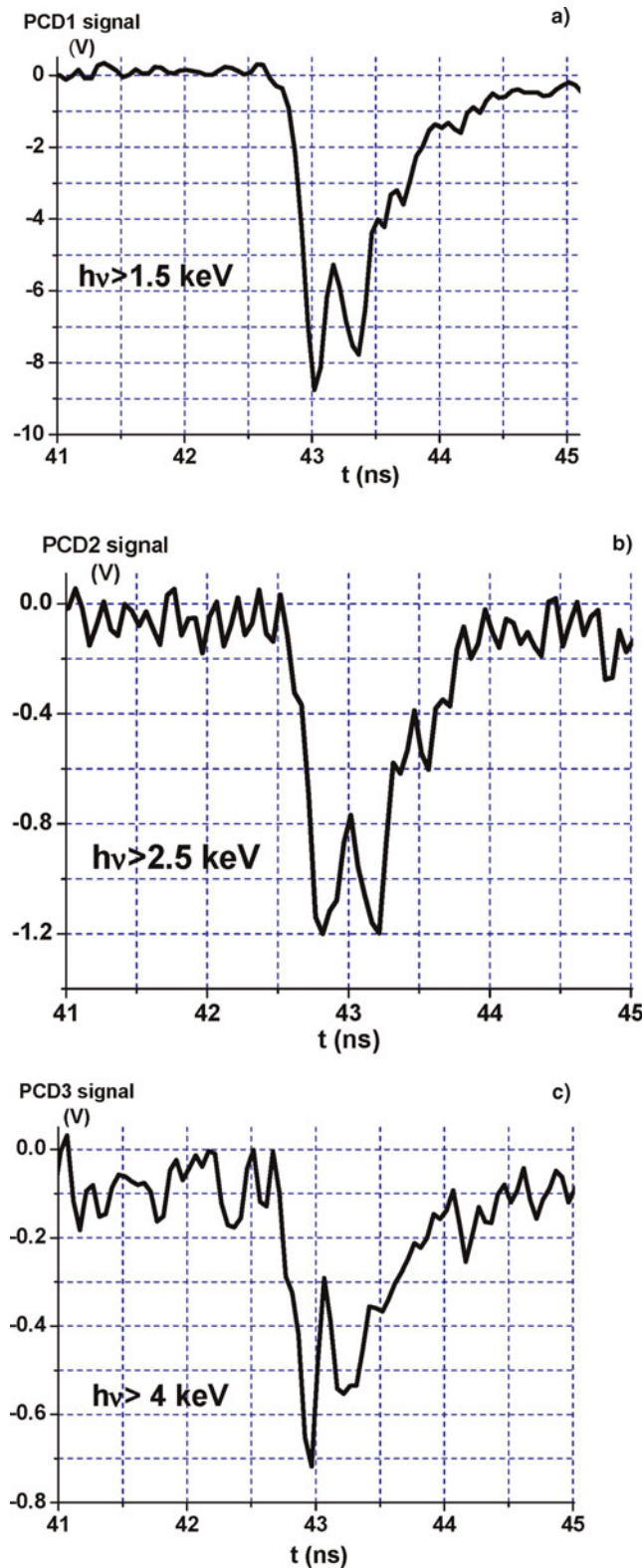


Fig. 3. (Color online) X-ray emissions in different ranges of photon energy (a) $h\nu > 1.5$ keV; (b) $h\nu > 2.5$ keV; (c) $h\nu > 4$ keV.

Based on an assumption that the X-ray emission is isotropic, the total X-ray energy emitted from the X-pinch could be calculated. It was found that the total X-ray energy changes

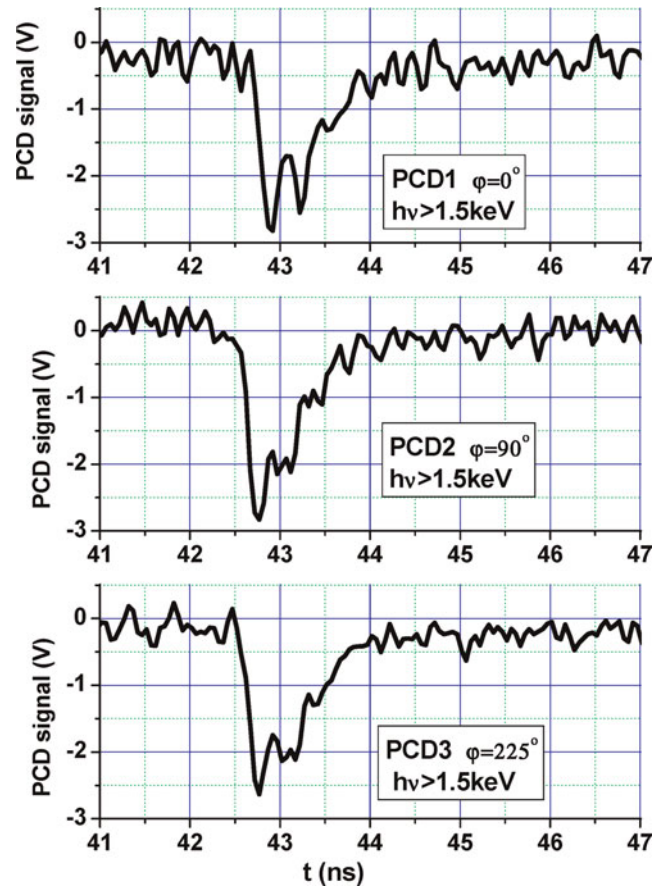


Fig. 4. (Color online) X-ray pulses recorded with three PCDs of the same filters.

from shot to shot and is averaged to be 0.35 J for $h\nu > 1.5$ keV. Since the mass of two 25- μm Mo wires seems too small for 200 kA load current, a heavier load consisting of two 50- μm Mo wires was tested and Figure 5 shows the results. In contrast to that shown in Figure 2a, the X-ray pulse in Figure 5a appears near the time when load current is maximal. There is only one single X-ray pulse with a pulse width of 0.5 ns in Figure 5b. The total X-ray energy calculated with the waveform of X-ray pulse of Figure 5b is 0.42 J.

3.2. Patterns of the X-ray Sources

Figure 6 are the typical X-ray pinhole pictures taken at same shot of X-pinch discharge using two 25- μm Mo wires as load. It was found from the pictures that there are usually two point sources of X-ray emission, which is consistent with the X-ray pulse with two peaks. These two point sources, with a distance of about 200 μm , are located near the crossing point of the two wires and along the axis of X-pinch load. It should be indicated that the effect of the pinhole size, 8- μm in diameter, must be taken into account when the source size is calculated basing on the pinhole pictures. The source size changes from about 100 μm to 8 μm dependent on the photon energy of the recorded X-rays.

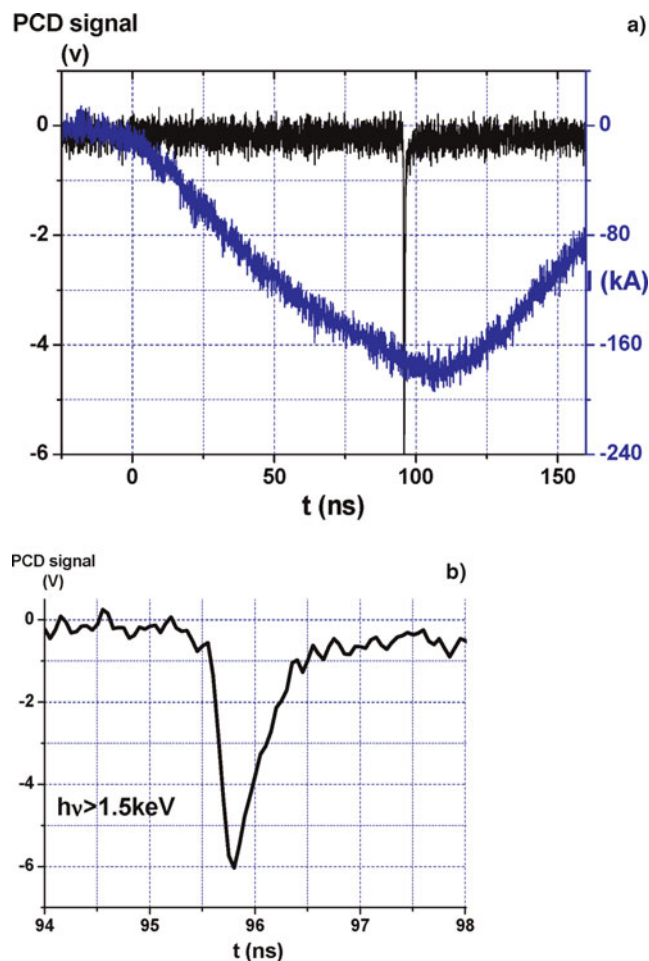


Fig. 5. (Color online) The typical result obtained from the experiments using two 50- μm Mo wires as X-pinch load: (a) The waveforms of the X-ray pulse and the load current, (b) the time expansion of the X-ray pulse.

In the case of using two 50- μm Mo wires as an X-pinch load, the typical pinhole picture is shown in Figure 7 in which two X-ray point sources, with sizes of 12 μm and 5 μm , are nearly overlapping.

3.3. X-ray Backlighting of the Electrical Explosion of Single Wire

In recent years, remarkable progress has been achieved in the X-ray generation of fast Z pinches (Deeney *et al.*, 1998), these X-ray generators are of great interest for inertial confinement fusion (ICF) and other high-energy density physics applications (Matzen, 1997). The key factor in this progress has been the use of cylindrical arrays with a large number (~ 400) of fine metallic wires as a Z-pinch load. Wire arrays provide a high degree of initial symmetry for the load and current distribution, which was thought to be able to lower the seed level for the development of Rayleigh–Taylor instabilities. However, the transition from metallic wires to plasma at the start of the current pulse

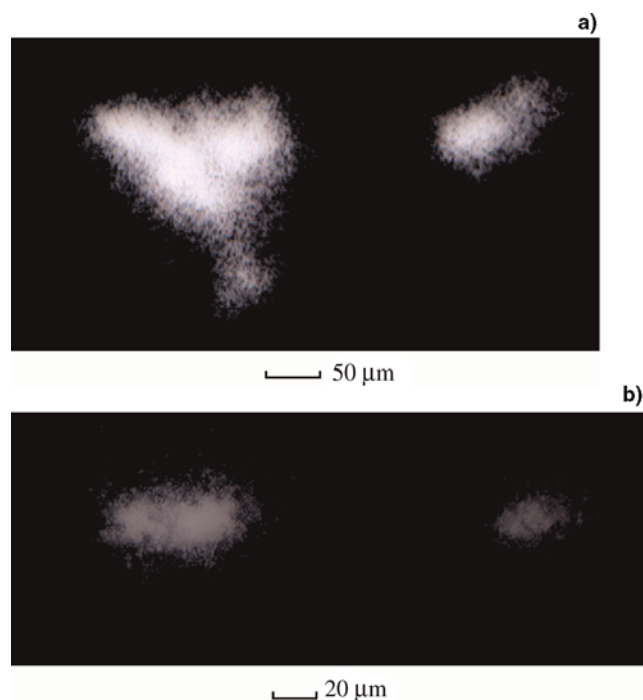


Fig. 6. (Color online) The pattern of the x-ray sources for two 25- μm Mo wires as a load, (a) $h\nu > 1.5$ keV; (b) $h\nu > 4$ keV.

and the mechanism responsible for inhomogeneity in mass distribution during the initial phase of the implosion need to be investigated. The transition from metallic wires to plasma and the mass distribution could be viewed by X-ray backlighting. X-pinch has proved to be a good X-ray source for backlighting (Lebedev *et al.*, 2001).

It was well known that the discharge of a wire array Z-pinch starts with an electrical explosion of each wire. As the first step of the investigation, we used X-pinch as X-ray

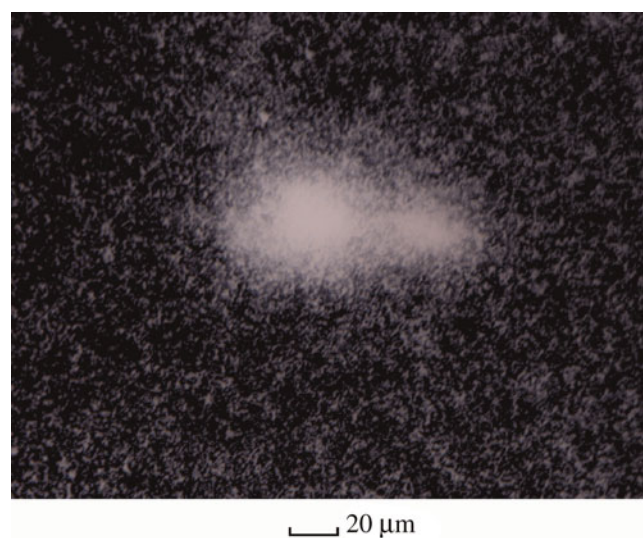


Fig. 7. (Color online) The pattern of the X-ray sources for $h\nu > 4$ keV in case of two 50- μm Mo wires as a load.

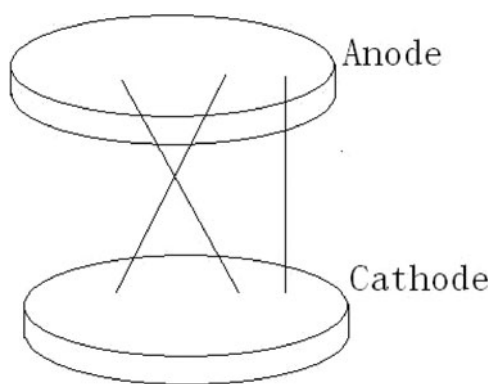


Fig. 8. Experimental arrangement using X-pinch as an X-ray source for backlighting of the electrical explosion of a single wire.

source to backlight the electrical explosion of a single wire. For the backlighting experiment, a new load of discharge was designed. The new load consists of one 200- μm Cu wire in parallel as a shunt with a two 25- μm Mo wires of X-pinch. As is shown in Figure 8, the electrical explosion of the Cu wire could be back-lighted by the X-ray emitted from the X-pinch.

With using this new load, the X-ray pulse of single sub-nanosecond peak appears at the time of current maximum, as was shown in Figure 9a. Two partly overlapping X-ray sources with a size of 5 μm to 10 μm for $h\nu > 4$ keV were usually observed, as shown in Figure 9b. Because the results obtained from using the new load are more stable, we use this load not only for the experiments in this subsection but also for the experiments in the next subsection.

Figure 10 is the picture from X-ray backlighting of the electrical explosion of 200- μm Cu wire. It could be seen that the high density wire core as well as the surrounding metallic plasma has expanded to a diameter much larger than 200 μm , the wire diameter before explosion.

3.4. X-ray Phase-Contrast Imaging of Mosquito

Phase-contrast radiography is different from the conventional radiography. While the conventional radiography relies on X-ray absorption as the sole source of contrast and ignores another and potentially more useful source of contrast, i.e., phase information, phase-contrast radiography records phase variations of X-rays passing through an object and offers improved contrast sensitivity, especially when imaging weakly absorbing samples (Fitzgerald, 2000). Wilkins *et al.* (1996) demonstrated a simplified scheme for phase-contrast imaging based on an X-ray source having high spatial coherence expressed by $d_{\perp} = \lambda l / \sigma$, where l is the source to observation distance, σ is the source size, λ is the wavelength of X-ray. Thus, high spatial coherence may be achieved by using a source having a small size or by observing the beam at a large distance from the source.

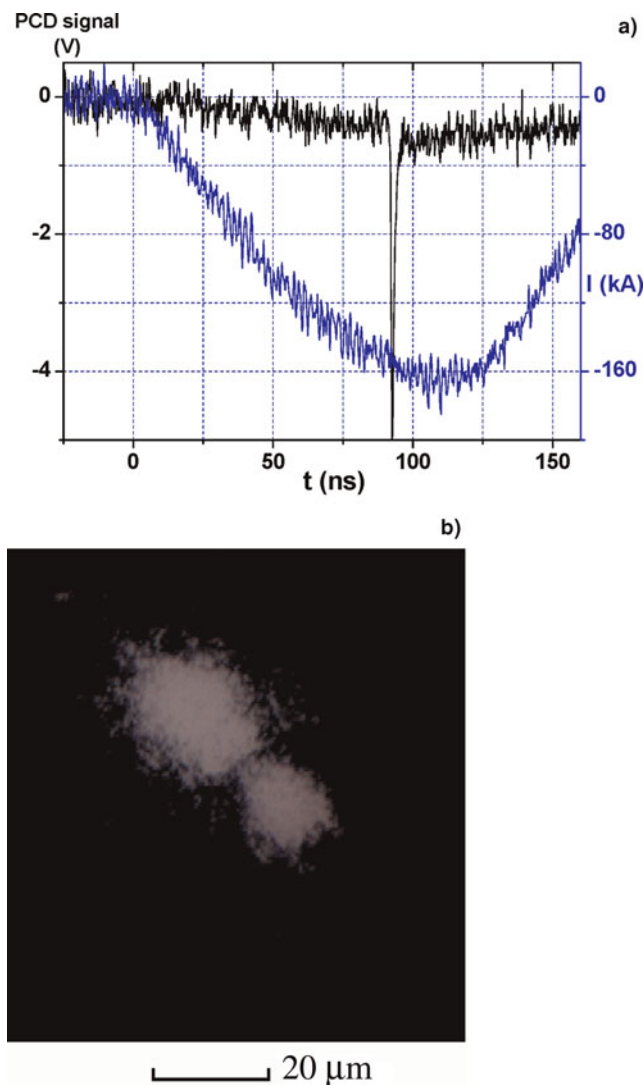


Fig. 9. (Color online) The typical result from the experiments using the load shown in Figure 8. (a) The waveforms of the X-ray pulse and the load current, (b) the pattern of the X-ray sources.

X-pinch X-ray source has advantages of high brightness and extremely small size, and it should be very suitable for X-ray phase-contrast imaging. Figure 11 shows the X-ray radiography of a mosquito using PPG-X as X-ray source. The picture was taken with a source-object distance of 220 mm and an object-image distance of 600 mm. Not only the small legs and fine feelers of the mosquito but also the structure and details inside the mosquito body could be clearly seen. This technique should find clinical and biological applications.

4. CONCLUSIONS

The temporal and spatial X-ray emission from PPG-X, an X-pinch, was studied by using three diamond photo-conducting detectors and pinhole cameras. It was found

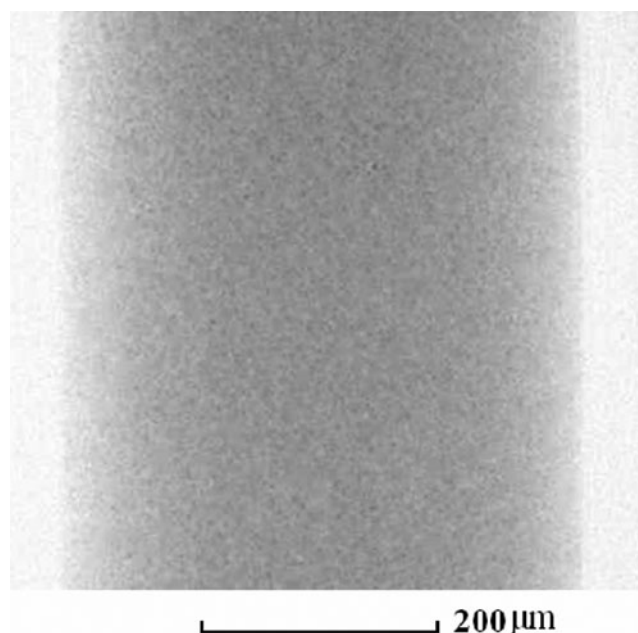


Fig. 10. Backlighting image of the electrical explosion of a 200- μ m Cu wire.

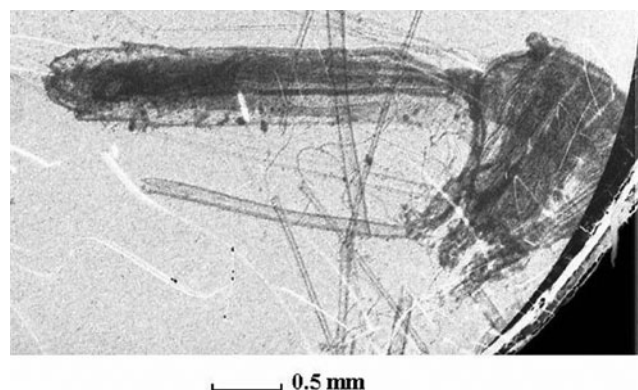


Fig. 11. Phase-contrast image of a mosquito using an X-pinch as X-ray source.

that the X-ray pulse usually consists of two sub-nanosecond peaks with a time interval of about 0.5 ns, these two X-ray peaks are consistent with two point sources of X-ray recorded with pinhole camera. The total X-ray energy changes from shot to shot and is averaged to be 0.35 J for $h\nu > 1.5$ keV. The size of the X-ray point source is in the range from 100 μ m to 5 μ m, decreasing rapidly with the increase of the photon energy. The X-pinch was used as X-ray source for backlighting the electrical explosion of single wire and for phase-contrast imaging of a mosquito.

ACKNOWLEDGEMENTS

This work was supported by National Natural Science Foundation of China under contracts 10635050, by Foundation for the Author

of National Excellent Doctoral Dissertation of PR China (FANEDD) under Contract No.200748, and by the International Atomic Energy Agency under research contract No.14509.

REFERENCES

- COSSLETT, V.E. & NIXON, W.C. (1960). *X-ray Microscopy*. London: Cambridge University Press.
- DEENEY, C., DOUGLAS, M.R., SPIELMAN, R.B., NASH, T.J., PETERSON, D.L., L'EPLATTENIER, P., CHANDLER, G.A., SEAMEN, J.F. & STRUVE, K.W. (1998). Enhancement of X-ray power from a z pinch using nested-wire Arrays. *Phys. Rev. Lett.* **81**, 4883–4886.
- FITZGERALD, R. (2000). Phase-sensitive X-ray imaging. *Phys. Today* **53**, 23–26.
- KANTSYREV, V.L., FEDIN, D.A., SHLYAPTEVA, A.S., HANSEN, S.B. & QUART, N.D. (2004). Characterization of the high-Z 0.9–1.0 MA X-pinch source in the 0.15–500 keV region: possible applications of the high-current X-pinch as the sub-keV–10 keV radiation driver and the 50–100 keV backlighter. *SPIE* **5196**, 45–56.
- LEBEDEV, S.V., BEG, F.N., BLAND, S.N., CHITTENDEN, J.P., DANGOR, A.E., HAINES, M.G. & ZAKAULLAH, M. (2001). X-ray backlighting of wire array Z-pinch implosions using X pinch. *Rev. Sci. Instr.* **72**, 671–673.
- LIU, J.L., LI, C.L., ZHANG, J.D., LI, S.Z. & WANG, X.X. (2006). A spiral strip transformer type electron-beam accelerator. *Laser Part. Beams* **24**, 355–358.
- LIU, J.L., YIN, Y., GE, B., ZHAN, T.W., CHEN, X.B., FENG, J.H., SHU, T., ZHANG, J.D. & WANG, X.X. (2007a). An electron-beam accelerator based on spiral water PFL. *Laser Part. Beams* **25**, 593–599.
- LIU, J.L., ZHAN, T.W., ZHANG, J., LIU, Z.X., FENG, J.H., SHU, T., ZHANG, J.D. & WANG, X.X. (2007b). A Tesla pulse transformer for spiral water pulse forming line charging. *Laser Part. Beams* **25**, 305–312.
- LIU, R., ZOU, X.B., WANG, X.X., HE, L.Y. & ZENG, N.G. (2008). X-pinch experiments with pulse power generator (PPG-1) at Tsinghua University. *Laser Part. Beams* **26**, 33–36.
- MATZEN, M.K. (1997). Z pinches as intense X-ray sources for high-energy density physics applications. *Phys. Plasmas* **4**, 1519–1527.
- ORLOV, N.Y., GUS'KOV, S.Y., PIKUZ, S.A., ROZANOV, V.B., SHELKOVENKO, T.A., ZMITRENKO, N.V. & HAMMER, D.A. (2007). Theoretical and experimental studies of the radiative properties of hot dense matter for optimizing soft X-ray sources. *Laser Part. Beams* **25**, 415–423.
- PLIDDEN, S.C., RICHTER, M.R., HAMMER, D.A. & KALANTAR, D.H. (1994). 1-kW X-pinch soft X-ray source. *SPIE* **2194**, 209–220.
- SPIELMAN, R.B. & DE GROOT, J.S. (2001). Z pinches: A historical view. *Laser Part. Beams* **19**, 509–525.
- WINTERBERG, F. (2006). Laser amplification by electric pulse power. *Laser Part. Beams* **24**, 525–533.
- WILKINS, S.W., GUREYEV, T.E., GAO, D., POGANY, A. & STEVENSON, A.W. (1996). Phase-contrast imaging using polychromatic hard X-rays. *Nature* **384**, 335–338.
- ZOU, X.B., LIU, R., ZENG, N.G., HAN, M., YUAN, J.Q., WANG, X.X. & ZHANG, G.X. (2006). Pulsed power generator for X-pinch. *Laser Part. Beams* **24**, 503–509.